Studying piezoelectric nanowires and nanowalls for energy harvesting

Christian Falconi [a,b,*], Giulia Mantini [a,c], Arnaldo D'Amico [a,b], Zhong Lin Wang [c,**]

[a] *Department of Electronic Engineering, University of Tor Vergata, Via del Politecnico 1, 00133 Rome, Italy*
[b] *CNR IDAC, Via Fosso del Cavaliere, 100, 00133 Rome, Italy*
[c] *School of Materials Science and Engineering, Georgia Institute of Technology, Atlanta, GA 30332-0245, USA*

ARTICLE INFO

ABSTRACT

Piezoelectric nanostructures can transduce mechanical energy into electrical energy for powering implantable microsystems for in-vivo biomedical applications (smart systems for drug delivery, μTAS, microsensors for diagnostic and therapeutic applications . . .) and sensors networks for high-density, low cost environment control. Zinc oxide nanowires and microwires have been recently used to convert vibrations into electrical energy. Here, we explain some previously reported experimental results and provide insight for the design of high-efficiency piezoelectric nanogenerators. Additionally, since the dimension and position of the electrical contacts, as well as the direction of the input force, can be very important, we define and systematically compare the most important configurations for 2-contacts piezoelectric nanowires; finally, we suggest that piezoelectric nanowalls can effectively increase the output currents. Our results are consistently confirmed by FEM simulations and can be a guidance for the design of high-efficiency energy harvesting devices and for the development of novel fabrication procedures.

© 2009 Elsevier B.V. All rights reserved.

1. Introduction

In principle, self-powered implantable microsystems might offer revolutionary opportunities in medicine; moreover, battery-free nodes of wireless sensors networks may enable high-density, low cost environment control (air quality, water quality; security in buildings, hospitals, bridges, roads, trains, airplanes . . .). Though conventional power supplies are restrictive for integration with microsystems, in principle, autonomous microsystems may harvest energy from the environment. Although the best "harvesting" strategy will always depend on the application, the mechanical to electric conversion by means of piezoelectric transducers is certainly one of the most promising options [1]. In particular, within the human body there are various mechanical energy sources which may, in principle, power implantable microsystems for in-vivo medical applications (e.g., heart beat, movements, blood flow . . .); as especially important examples, these in-body mechanical energy sources may power smart systems for drug delivery, implantable μTAS, and microsensors for facilitating diagnosis as well as for closed loop therapies.

Recently, zinc oxide nanowires have been used for transducing vibrations into electric energy [2]; interestingly, it is possible to integrate an enormous number (e.g., billions per square centimeter) of piezoelectric nonotransducers on a single substrate.

In order to effectively harvest mechanical energy, many practical issues must be considered: how the piezoelectric potential can be simultaneously generated in a large number of nanowires; how the electric energy can be extracted and applied to an external load; how the nanostructures and the microsystem can be fabricated, assembled, and packaged. A first solution [3–5] to all these practical problems has taken advantage of a zig-zag, Pt-coated, silicon top electrode and of Schottky barriers between nanowires and the top electrode; afterwards, the microfibre-nanowire hybrid structure [6] and, more recently, laterally stretched microwires have been reported [7]; the physics for nanogenerators has been reviewed elsewhere [8–9]. However, key issues have not yet been satisfactorily addressed, namely the way the force is applied and the importance of the contacts.

Obviously, the critical challenge for energy harvesting is high-efficiency. As we mentioned, various issues must be solved in order to power a microsystem by means of piezoelectric nanostructures; moreover, the overall efficiency of the complete system will, in general, depend on many parameters. However, in this paper, without regard to technological or practical issues, we exclusively focus on the conversion of a given static force into a voltage based on theoretical calculation. With this approach, we consider both previously reported and novel piezoelectric nanostructures for energy harvesting and systematically compare their output potentials when

* Corresponding author at: Department of Electronic Engineering, University of Tor Vergata, Via del Politecnico 1, 00133 Rome, Italy.
** Corresponding author.
E-mail addresses: falconi@eln.uniroma2.it (C. Falconi),
zhong.wang@mse.gatech.edu (Z.L. Wang).

a given static force is applied; both theoretical considerations and FEM (finite element method) simulations allow the identification of the optimal nanostructures (from the point of view of the output voltage for a given input force). In particular, in case of a lateral force applied to the free tip of a nanowire, the presence of continuous conductive films at the base of the nanowire (i.e. in the high-strain region) can significantly reduce the output potential; by contrast, in case of vertical compression or lateral stretching, since the strain is more uniformly distributed, the presence of continuous conductive films at the base and/or tip does not significantly reduce the output potential; this observation explains the practical advantages of laterally stretched microwires, in agreement with the experimental results in [7].

Finally, we suggest that nanowalls [10] can replace nanowires in order to increase the maximum output current.

For all the FEM simulations, for simplicity, without loss of generality, we consider zinc oxide as the piezoelectric material; moreover, we neglect its electrical conductivity and we restrict our attention to static simulations. Our focus will be the estimation of the output potential and stored electrostatic energy under various deformation configurations and with different positions of the contacts. These assumptions can be tolerated as our goal is to qualitatively compare the potentialities of different nanostructures and provide insight for the design of high-efficiency piezoelectric nanostructures, rather than quantitatively predict the piezoelectric potential output; besides, our results can be a good start for the development of more sophisticated models.

It is important to observe that, though efficiency is the key performance of energy harvesting devices, it is currently impossible to compute the efficiency of nanogenerators and, for this reason, simplified criteria must be adopted. In fact, current methodologies for the analysis of nanogenerators [8] are limited to static parameters; however, dynamic parameters (capacitances and, more in general, impedances) are certainly significant; even more important, nanogenerators are non-linear devices (because of the Schottky barriers between nanowires and contacts); finally, the output power of nanogenerators can only be calculated for a given external circuit. For these reasons, in order to classify and compare different structures, we compute the static output potential, electrostatic and strain energies for all the relevant structures; then, if we consider a certain input force, structures with high static output potential and high electrostatic energy seem good candidates for energy harvesting and vice versa. The results obtained with this obvious criterion are consistent with experimental results in [7], as discussed in the paper.

Clearly, after the identification of the nanostructures with good properties for energy harvesting, practical methods for fabricating the correspondent arrays of nanogenerators must be found. Until now a variety of methods for fabricating arrays of aligned ZnO nanowires has been reported, including vapor phase transport, metal-organic chemical vapor deposition (MOCVD), hydrothermal synthesis and wet chemical method. In particular, the wet chemical method allows to obtain a density-controlled growth of aligned ZnO nanowires; in practice, a Si substrate is covered with gold on one face and immersed (face down) in a proper nutrient solution at a desired temperature in order to promote the nanowires growth. In the solid vapor process, condensed or powder source materials are vaporized at high temperatures and then the resultant vapor phases condense under certain conditions to form the desired products (this process is usually carried out in a horizontal tube furnace). Obviously, such simple methods do not allow the simultaneous fabrication of appropriate contacts and more elaborate methodologies may be necessary. It may therefore be difficult to build practical nanogenerators based on an arbitrary theoretical configuration. For this reason FEM simulations can be very important. In fact, the goal of this paper is to offer insight for the design of nanogenerators

and to guide the development of procedures for the fabrication of improved nanogenerators.

It is also important to observe that piezoelectric nanogenerators are "wireless nanotransducers" [11–13], a broad class of nano-sized transducers which can be especially important for in-vivo medical applications (e.g., see gold nanoshells [14–15]); in particular, nanogenerators could wirelessly transduce mechanical vibrations into electric energy for powering implantable microsystems.

This paper is organized as follows. In Section 2 we classify the most important positions of the contacts and piezoelectric nanostructures for lateral bending, vertical compression and lateral stretching and, as an important example, we apply these classifications to nanowires. In Section 3 we use FEM simulations in order to systematically compare the output potential, electrostatic energy and strain energy of the most important nanowires for energy harvesting. In Section 4 we propose piezoelectric nanowalls for energy harvesting and extend to nanowalls the results obtained in Sections 2 and 3. The conclusions are drawn in Section 5.

## 2. Classification of piezoelectric nanostructures for energy harvesting

Since we will consider nanostructures vertically grown on a substrate, we can unambiguously refer to their "bottom" and "top" parts (i.e., the bottom part is the one in contact with the substrate); accordingly, we will also refer to their "base" and "tip" (e.g., the "base" is the interface between the nanostructure and the substrate). We observe that even in case of vertical compression and lateral stretching, it is still possible to distinguish between top and bottom (i.e., tip and base) depending on the nanostructure growth process.

A piezoelectric nanostructure for energy harvesting must necessarily include two electrical contacts to be connected to the load; in the rest of this section we classify the most important contacts positions for lateral bending, vertical compression, and lateral stretching.

We stress that, in practice, differences between the two contacts may be critical for proper operation; as an example, in nanogenerators, the nanowire and one of the two contacts must behave as a Schottky barrier, while the nanowire and the other contact must behave as an ohmic contact [9]. However, even if the unsymmetrical nature of the two contacts may be crucial, we will simply consider two identical metal contacts, as our goal is simply to estimate the piezoelectric potential generated by mechanical forces.

2.1. Lateral bending

In case of lateral bending with a force applied at the free tip of the nanowire, the position of the contacts critically affects the output potential and, therefore, it is convenient to classify different structures depending on the positions of their electrical contacts. For this reason, we will refer to *c1–c2* nanostructures if the electrical contacts are in the *c1* (top or bottom) and *c2* (top or bottom) position; as an example, a top-bottom nanowire has one electrical contact at the top and the other one at the bottom. For practical reasons we restrict to the top and bottom positions of contacts (bottom contacts can be located on the substrate or can even be the substrate itself; top contacts can be added as, e.g., in [2,7]); beside these practical reasons, top-bottom configurations are also the most convenient for vertical compression and lateral stretching (almost uniform strain), while top-bottom and bottom-bottom configurations are sufficient for investigating lateral bending (as the strain is maximum at the bottom); moreover, our results can allow a qualitative prediction of the results for other possible configurations.
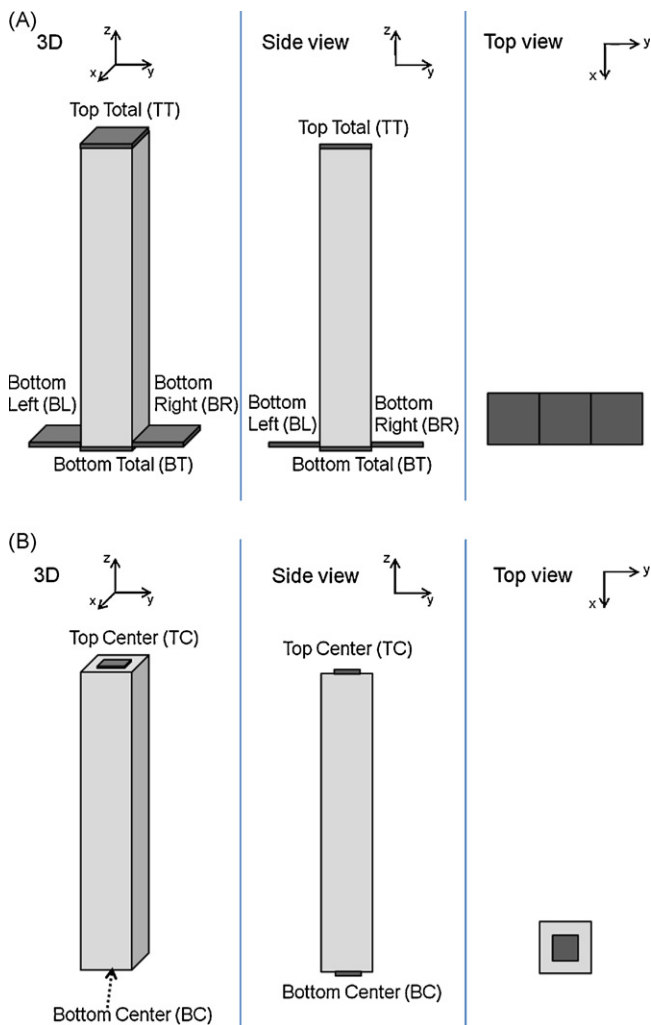
Fig. 1. (A) Definition of top-total (TT), bottom left (BL), bottom right (BR), and bottom total (BT) contacts. (B) Definition of bottom center (BC) and top-center (TC) contacts.

For nanostructures vertically aligned on a substrate, for practical reasons, at least one of the two contacts should be at the bottom, so that the possible contacts configurations are top-bottom and bottom-bottom. With reference to Fig. 1, in principle, both at the top and at the bottom, left, right, total, or center contacts are possible. As additional important possibilities, electrical contacts can be so small that they do not significantly perturb the potential distribution inside the nanowire; in these cases, for simplicity, we will refer to "negligible" contacts; for instance, a "top-negligible" contact in a "top-bottom nanowire" is a top contact so small that its presence does not significantly affect the potential distribution (clearly, this so called "negligible contact" is actually "essential" for connecting to the load). This qualitative definition is preferred because a quantitative definition would be unnecessarily complex and confusing (in fact the effects of a contact depend on both its dimensions and its position).

In case of lateral bending with force applied at the free tip of the nanowire, since the high-strain regions are at the bottom, it is necessary to explicitly consider all of the possibilities for the bottom contacts. As to the top contacts, if we explicitly consider only the top-total, the top-center, and the top-negligible configurations, other possibilities can be easily (qualitatively) evaluated. As a result, for lateral bending, it is convenient to explicitly consider the six contacts shown in Fig. 1A (bottom-left, BL; bottom-right, BR; top-total, TT; bottom-total, BT) and 1B (top-center, TC; bottom-center,

BC) and the two additional "negligible" top and bottom contacts (bottom-negligible, BN; top-negligible, TN).

Beside the "true contacts" necessary for connecting to the load, other conductive films can be deliberately (e.g., a conductive film on the substrate) or not (e.g., non-ideal fabrication steps) deposited on the nanostructure or on the substrate; for simplicity it is convenient to refer to such conductive films as additional "contacts". In general, additional contacts in the middle of the nanostructure (i.e., far away from both the base and the tip) are relatively unimportant as they would be far from both high-strain regions and the "true contacts". However, it can be important to consider the possible presence of these additional contacts at the tip or at the base of the nanowire.

In summary, for the top-bottom configurations, we will consider for the top contact all the possibilities TN, TC, TT; for the bottom contact, we can restrict our attention to BN (from this case the BL and BR configurations can be easily deduced), BC, and BT contacts, resulting in nine top-bottom configurations. For the bottom-bottom configurations, the best positions for the two contacts are, obviously, bottom-left (BL) and bottom-right (BR); with this choice, additional top contacts (TN, TC, TT) and/or bottom contacts (BN, BC, BT) are possible, resulting in nine bottom-bottom configurations. The 18 configurations which will be explicitly discussed are then as follows:

TN–BT piezoelectric nanowires
TT–BT piezoelectric nanowires
TC–BT piezoelectric nanowires
TN–BC piezoelectric nanowires
TT–BC piezoelectric nanowires
TC–BC piezoelectric nanowires
TN–BN piezoelectric nanowires
TT–BN piezoelectric nanowires
TC–BN piezoelectric nanowires
BL–BR piezoelectric nanowires
BL–BR piezoelectric nanowires with TT contact
BL–BR piezoelectric nanowires with TC contact
BL–BR piezoelectric nanowires with BC contact
BL–BR piezoelectric nanowires with BC contact and TT contact
BL–BR piezoelectric nanowires with BC contact and TC contact
BL–BR piezoelectric nanowires with BT contact
BL–BR piezoelectric nanowires with BT contact and TT contact
BL–BR piezoelectric nanowires with BT contact and TC contact

Though other types of contacts are possible (i.e., a top-left contact), these 18 configurations are, in practice, sufficient for a qualitative understanding of what would happen with arbitrary positions of the contacts.

Among the 18 configurations listed above, all of the bottom-bottom configurations with additional BT contacts are, clearly, useless, as the voltage between the two "true contacts" (BR and BL) would, obviously, be zero (see Fig. 1A); as a result the analysis of the remaining 15 configurations is sufficient for lateral bending.

According to the proposed classification, piezoelectric nanogenerators [3–5] are likely to behave as top-bottom ZnO nanowires with a BT contact [2] made of the continuous conductive film underlying all the nanowires; this continuous conductive film is, obviously, necessary as it implements the bottom electrode of nanogenerators. The tips of different nanowires in the array can present TN, TT, or TC contacts; the nanowires with TT contact did not allow the detection of an output voltage [2], in agreement with the theoretical analysis given in Section 3.5.

2.2. Vertical compression

In case of vertical compression the position of the contacts is obvious as the simplest choice (one "total contact" at the base and

another "total contact" at the tip) is also the most convenient; with reference to Fig. 1A, it is therefore sufficient to consider "total" bottom and top contacts (TT–BT) and the input force are parallel to the axis z.

2.3. Lateral stretching

As in the case of vertical compression, in case of lateral stretching [7] the position of the contacts is obvious as the simplest choice (one "total contact" at the base and another "total contact" at the tip) is also the most convenient; with reference to Fig. 1A, it is therefore sufficient to consider "total" bottom and top contacts (TT–BT) and the input force is parallel to the axis y.

3. FEM calculations

In this section we consider the most important piezoelectric nanostructures for energy harvesting, as described in Section 2; for all of the cases of lateral bending, vertical compression, and lateral stretching we give the results of 3D FEM simulations performed on ZnO nanowires. Top-bottom ZnO nanowires with BT contact and lateral bending will be considered first, as these results (consistent with [8]) will be useful for comparison.

The electrostatic energy U has been calculated according to the formula:

$$U_{\text{electrostatic}} = \int_{\text{volume}\Omega} \frac{1}{2} \varepsilon E^2 d\Omega \qquad (1)$$

where ε is the dielectric constant, E is the intensity of the electric field and Ω is the volume of the structure. The strain energy (reported in Table 1 for all the structures) has been calculated according to the formula:

$$U_{\text{strain}} = \int_{\text{volume}\Omega} \frac{1}{2} (\sigma_x \varepsilon_x + \sigma_y \varepsilon_y + \sigma_z \varepsilon_z + \tau_{xy} \gamma_{xy} + \tau_{yz} \gamma_{yz} + \tau_{xz} \gamma_{xz}) d\Omega \qquad (2)$$

where σ_i and γ_{ij} are the normal and shear stress, respectively and ε_i and τ_{ij} are the normal and shear strain.

The parameter ξ has been defined as

$$\xi = \frac{U_{\text{electrostatic}}}{U_{\text{strain}}} \qquad (3)$$

ξ does not simply coincide with the efficiency of the nano-transduction process as it only refers to static simulations (once

a nanowire is deflected by an external force and then left free to move, it will experience many cycles of vibrations at its resonance frequency before it totally stops, and in each cycle of the vibration, electricity will be generated); besides, only a fraction of the stored electrostatic energy can effectively be extracted (as an extreme example, the output potential of a bottom-bottom nanowire with a BT contact will always be zero and no energy can be delivered to an external load, no matter how much energy is stored in the nanowire).

For the FEM simulations of TN–BT nanowires we have considered a cylindrical nanowire, in accordance with [8]. For simplicity, for all the other nanowires, we have considered a "square base" nanowire, as this choice is more convenient for configurations requiring lateral contacts (clearly, the simulation of a top-bottom ZnO nanowire with a "square base" BT contact would give, practically, the same results as the simulation with "circular base").

In all the simulations of laterally bent nanowires, we have used the same lateral surface force (40×10^6 N/m²); the results will be summarized in Table 1. Similar to [8], the FEM calculations have been carried out considering the fully coupled electromechanical system; the parameters for the anisotropic elastic modulus tensor, relative dielectric constants and piezoelectric constants have been taken from [8] (considering the C_6v symmetry of the ZnO crystal with wurtzite structure); all the calculations have been carried out for c-axis vertically aligned ZnO nanowires.

FEM calculations have been performed with the COMSOL Multiphysics software.

3.1. Top-bottom piezoelectric nanowires with BT contact

3.1.1. TN–BT piezoelectric nanowire

Similar to [8], a nanowire with cylindrical geometry (50 nm diameter and 600 nm length) has been laterally deflected by a lateral bending force of 80 nN; the force has been applied to the top surface of the nanowire in order to avoid punctual deformations [8], which result, in practice, in the application of a surface force approximately equal to 40×10^6 N/m². The bottom surface was affixed and entirely grounded (BT contact). The nanowire has been considered as an ideal dielectric medium (i.e., its electrical conductivity is zero). Fig. 2a shows the potential distribution viewed from side (this simulation is in excellent agreement with [8] and, in particular, shows the parallel plate capacitor model of piezoelectric potential [8]). The electrostatic energy is about 7.02×10^{-18} J; the strain energy is about 5.13×10^{-15} J.

Table 1
Results for all configurations presented: contact position, output potential, electrostatic and strain energy, ξ parameter and paragraph where the configuration has been presented.

	Electrodes	Tip	Base	V_{out}^* (V)	$U_{\text{electrostatic}}$ [J]	U_{strain} [J]	ξ	Par.
1	Top-bottom	TN	BT	−0.3 to 0.3	7.02×10^{-18}	5.13×10^{-15}	0.00137	3.1.1
2	Top-bottom	TT	BT	0	7.02×10^{-18}	4.78×10^{-15}	0.00147	3.1.2
3	Top-bottom	TC	BT	0	6.97×10^{-18}	4.61×10^{-15}	0.00151	3.1.3
4	Bottom-bottom	TN	BL + BR	~6	4.47×10^{-17}	4.45×10^{-15}	0.0100	3.2.1
5	Bottom-bottom	TT	BL + BR	~6	4.59×10^{-17}	4.68×10^{-15}	0.0098	3.2.2
6	Bottom-bottom	TC	BL + BR	~6	4.50×10^{-17}	4.51×10^{-15}	0.0099	3.2.3
7	Bottom-bottom	TN	BL + BR + BC	~4	3.07×10^{-17}	4.47×10^{-15}	0.0069	3.4.1
8	Bottom-bottom	TT	BL + BR + BC	~4	3.08×10^{-17}	4.7×10^{-15}	0.0065	3.4.2
9	Bottom-bottom	TC	BL + BR + BC	~4	3.05×10^{-17}	4.53×10^{-15}	0.0067	3.4.2
10	Top-bottom	TN	BC	−0.3 to +0.3	3.32×10^{-17}	4.55×10^{-15}	0.0073	3.5
11	Top-bottom	TT	BC	0	3.34×10^{-17}	4.78×10^{-15}	0.0070	3.5
12	Top-bottom	TC	BC	0	3.32×10^{-17}	4.6×10^{-15}	0.0072	3.5
13	Top-bottom	TN	BN		Same as #4			3.3
14	Top-bottom	TT	BN		Same as #5			3.3
15	Top-bottom	TC	BN		Same as #6			3.3
16	Top-bottom z-compression	TN or TT	BT	−2.5	9.24×10^{-19}	6.69×10^{-18}	0.138	3.6
17	Top-bottom lateral stretch	TT	BT	3.7	2.65×10^{-18}	4.48×10^{-17}	0.059	3.7

* The output potential is the one obtained between the electrodes listed in column 2.
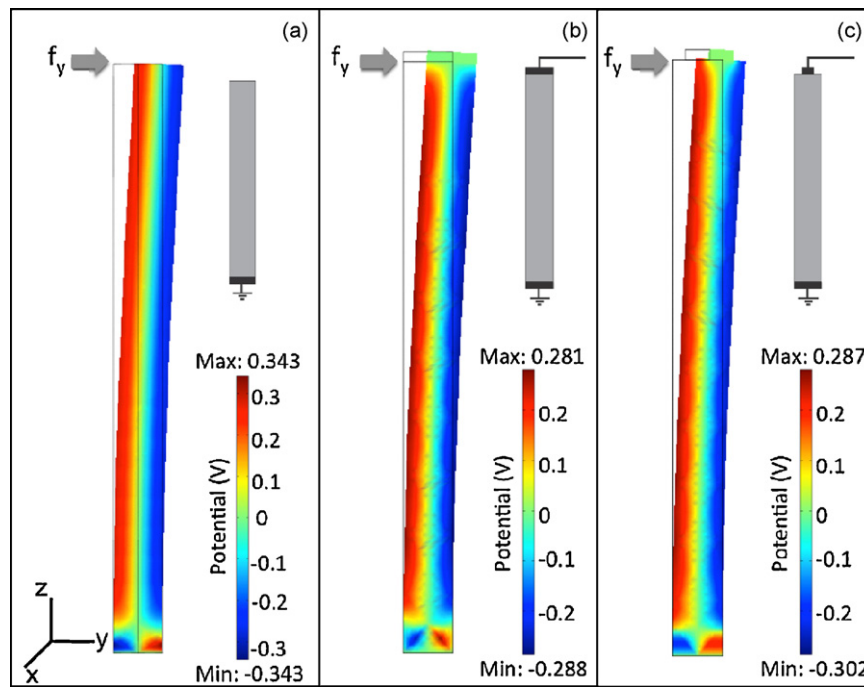
Fig. 2. Piezoelectric potential distribution (side view) in a top-bottom ZnO nanowire: TN–BT (a), TT–BT (b), TC–BT (c).

We did not explicitly add the metal contact at the tip (i.e., we used a TN contact); the tip potential varies from −0.3 to +0.3 V and can drive a discharge process when a Schottky barrier is created between the nanowire and the metal tip of an AFM, as described in [2]. Clearly, if a small metal contact (TN) is used at the tip in order to deliver electrical energy to an external load, it may not significantly change the electric potential distribution illustrated in Fig. 2a; on the contrary, if a very large metal contact (e.g., TT contact) is added at the tip, the electrical potential distribution can be significantly perturbed (e.g., see Fig. 2b).

Apart the simulation shown in Fig. 2a (which, coherently with [8] takes into account a cylindrical nanowire), all other simulations refer to "square base" nanowires (50 nm side, 600 nm height) because the square geometry is more convenient for lateral contacts simulations. The lateral bending force is the same as for the first simulation (40×10^6 N/m^2); the results for a top-bottom ZnO nanowire with a "square" BT contact would be almost identical to those shown in Fig. 2a.

3.1.2. TT–BT piezoelectric nanowires

Fig. 2b shows the potential in the bent nanowire when both a BT contact and a TT contact are present (the metal contact dimensions are 50 nm × 50 nm and 10 nm height) and the BT contact is grounded. The electrostatic energy is 7.02×10^{-18} J; the strain energy is 4.78×10^{-15} J. The output potential between the top and bottom contacts is 0 V. This result is consistent with experimental results reported in [2] (the nanowires with a large Au particle at the top did not produce a measurable output voltage) and can be easily explained. In fact, the base voltage is constant and equal to zero because the BT contact is grounded; the tip voltage is also constant as the tip also contains a TT contact; moreover, the electric potential along the axis of the nanowire is constant (symmetry); the voltage difference between the tip and the base is therefore zero. This result, obviously, only holds for lateral bending with force applied at the free tip of the nanowire.

3.1.3. TC–BT piezoelectric nanowires

Fig. 2c shows the potential in the bent nanowire when a BT contact and a TC contact are present (the dimensions of the TC metal contact are 25 nm × 25 nm and 10 nm height) and the BT contact is grounded. The electrostatic energy is 6.97×10^{-18} J; the strain energy is 4.61×10^{-15} J. Similar to the previous configuration, the output potential between the top and bottom contacts is 0 V (see discussion in Section 3.1.2). However, if the top contact is smaller and not at the center of the tip, it becomes possible to obtain a discharge process, due to the forward biased Schottky diode, as described in [2].

3.2. Bottom-bottom piezoelectric nanowires without additional base contacts
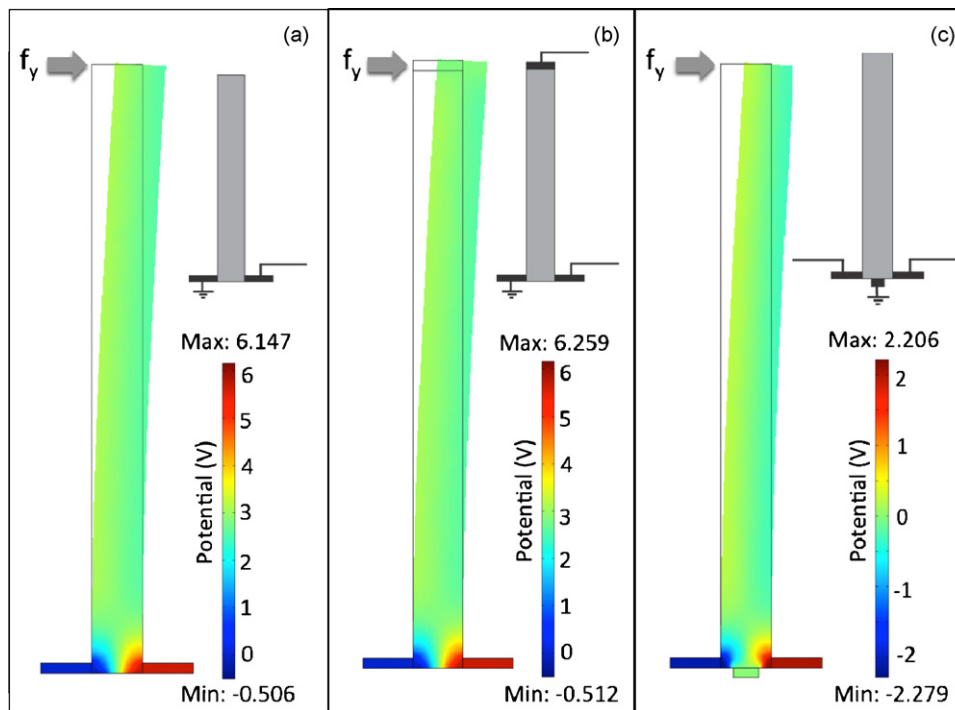
3.2.1. BL–BR piezoelectric nanowires

A bottom-bottom square base nanowire has been considered and bent by the same force as before. The two identical gold contacts have been placed laterally at the base of the NW; the BL contact has been grounded. All the other parameters were the same as in the previous calculations.

Fig. 3a shows the potential distribution; the output potential between the BL and BR contacts is about 6 V; the electrostatic energy is 4.47×10^{-17} J and the strain energy is 4.45×10^{-15} J. Both the voltage and the electrostatic energy are significantly higher than the correspondent values of the top-bottom ZnO nanowire with BT contact. In fact, in this configuration, the regions subject to the highest strain (i.e., the bottom part of the nanowire) are not covered by conductive films. In fact, FEM simulations consistently confirm (see later) that nanowires with BT contact are not optimal from the point of view of the output potential generated by lateral bending; clearly, in some cases, technological issues might favor the use of sub-optimal nanostructures.

3.2.2. BL–BR piezoelectric nanowires with TT contact

Fig. 3b shows the same simulation when a top Au TT contact is added at the tip of the nanowire (the boundary conditions

Fig. 3. Piezoelectric potential distribution (side view) in a bent bottom-bottom nanowire with various configurations: BL (grounded)–BR (a); BL (grounded)–BR with TT contact (b); BL–BR with TC (grounded) contact (c).

are the same as in the calculation without the top electrode). The piezoelectric potential is 6 V, as in the configuration without top electrode. The electrostatic energy for this configuration is 4.59×10^{-17} J, very similar to that obtained without the top electrode. The strain energy is 4.68×10^{-15} J. Fig. 4a and b shows the same simulations when, respectively, only the BL contact is considered and when an additional metal film is positioned at

Fig. 4. Piezoelectric potential distribution (side view) in a bent bottom-bottom nanowire: BL (grounded)–TT (a); BL (grounded)–BC with TT and middle contact (b).

the middle of the nanowire. With reference to the simulation in Fig. 4a, the output potential between the BL and the TT contacts is about 3 V. All these simulations also demonstrate that spurious metal films, which are far from the high-strain regions, do not significantly reduce the piezoelectric potential; this can be an important result for the determination of practical fabrication procedures.

3.2.3. BL–BR piezoelectric nanowires with TC contact

With the BL contact grounded, simulation results are almost identical to those described in Sections 3.2.1 and 3.2.2.

3.3. Top-bottom piezoelectric nanowires without bottom contact

This section includes three top-bottom configurations with BN contact and with TN, TT or TC contact. The results are almost the same as the correspondent bottom-bottom simulations (i.e., bottom-bottom ZnO nanowires with BN contact) and are therefore not separately shown. In particular, the simulation of a TT–BN ZnO nanowire gives, obviously, the same results as shown in Fig. 3b and therefore also confirms that when a nanowire is bent, if the base of the nanowire is not totally in contact with conductive materials, the piezoelectric potential of the nanowire can be significantly higher.
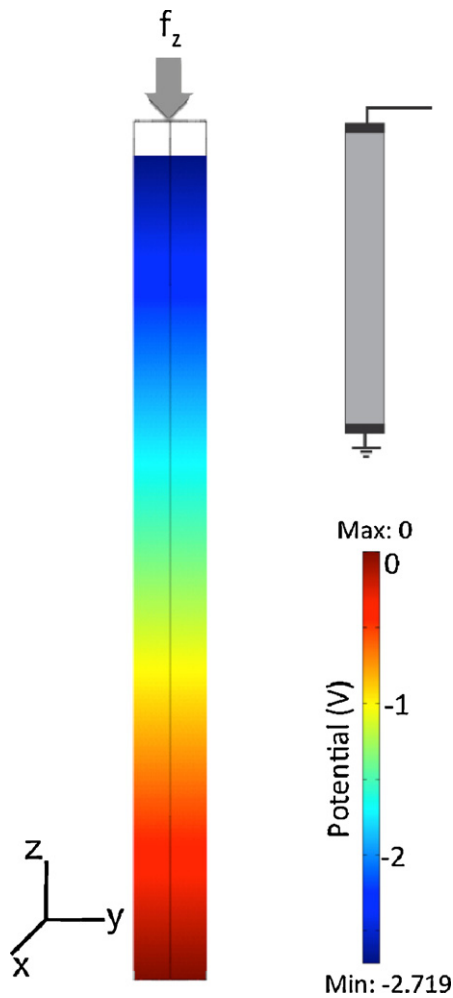
3.4. Bottom-bottom piezoelectric nanowires with BC contact

3.4.1. BL–BR piezoelectric nanowire with BC contact

Fig. 3c shows the simulation of the bent nanowire when the BC contact is present (the metal contact 25 nm × 25 nm and 10 nm height) and grounded; the piezoelectric potential between the BL and BR contacts is about 4 V, which is lower if compared with a correspondent structure without the BC contact, but is not zero (as it would happen with a BT contact). The electrostatic energy is 3.07×10^{-17} J and the strain energy is 4.47×10^{-15} J.
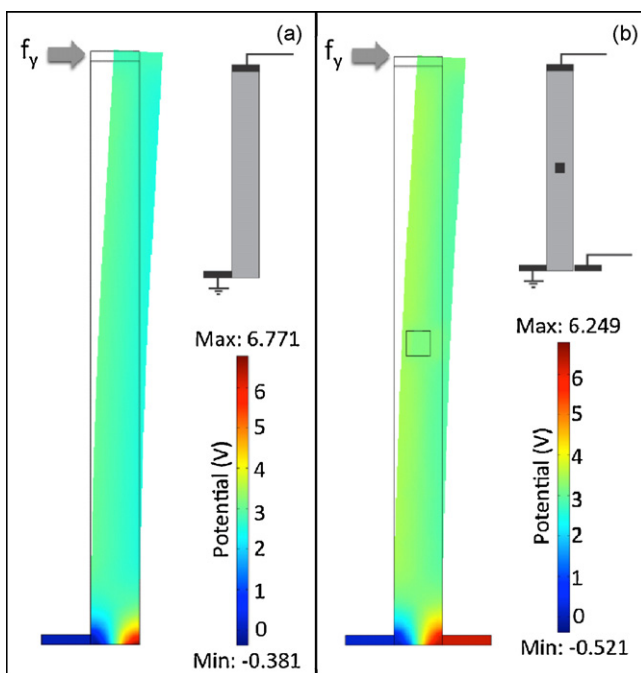
Fig. 5. Piezoelectric potential distribution (side view) in a compressed top-bottom nanowire (base totally short-circuited and base grounded).

3.4.2. BL–BR piezoelectric nanowire with BC contact and with TT or TC contact (two configurations)

With the same boundary conditions, both these simulations give results almost identical to those shown in Fig. 3c for the bottom-bottom ZnO nanowire with BC contact and without tip contact.

3.5. Top-Bottom piezoelectric nanowires with BC contact

With the same boundary conditions, for all these three configurations (with TN, TC or TT contact), the results are almost the same as those of the bottom-bottom ZnO nanowires with BC contact and are, therefore, not explicitly shown here.

3.6. Top-Bottom piezoelectric nanowire with vertical compression

All the previous simulations assume a lateral bending with force applied at the free tip of the nanowire; it is, however, possible to apply a vertical compressive force (i.e., parallel to the axis of the nanowire). Contrary to lateral bending forces (see discussion in Section 3.1.2), in this case, obviously, the electric potential along the central axis of the nanowire is not constant; for this reason, a high output potential can be generated even when both the base and the tip are totally covered by conductive materials, a potentially critical advantage for practical implementations.

Fig. 5 shows the potential in a ZnO nanowire when a force is applied in the z direction; the NW is compressed and a negative potential of about 2.5 V is generated between the top surface of the NW and the grounded base. The electrostatic and strain energy for this configuration are 9.24×10^{-19} and 6.69×10^{-18} J, respectively; though the strain energy is significantly lower than the correspondent energy related to lateral bending, the parameter ξ is significantly higher.

3.7. Laterally packaged top-bottom piezoelectric nanowire

As presented in [7], a laterally packaged piezoelectric wire has been developed as power generator. This configuration presents two "total" metal contacts at both ends, and it is indeed similar to the top-bottom nanowires presented in the previous sections; however, in this configuration, a bending force is applied in order to stretch the whole piezoelectric wire (instead of fixing one end and applying a lateral bending force to the free end). In this manner, the strain is more uniformly distributed along the structure and, therefore, using "total contacts" at the two ends does not significantly reduce the output piezoelectric potential, a striking advantage for practical implementations.
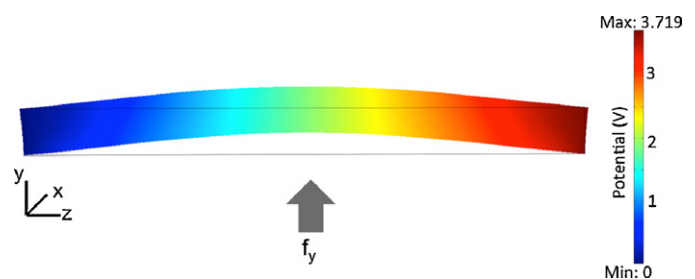
Fig. 6 shows the piezoelectric potential distribution of a laterally stretched ZnO nanowire with the left, total contact of the nanowire grounded. For the sake of comparison, the dimensions of the wire are the same as that in the previous sections. The applied surface force on the lateral face is 3.33×10^6 N/m^2 and has been chosen in order to obtain the same punctual force of the lateral bending configurations.

The electric potential generated between the top and bottom (grounded) metal contact is about 3.7 V. The electrostatic and strain energy for this configuration are 2.65×10^{-18} and 4.48×10^{-17} J, respectively.

3.8. Comments on nanowires piezoelectric nanogenerators

The results for all of the 15 meaningful configurations with lateral bending are summarized in the first 15 rows of Table 1 (bottom-bottom configurations with BT contact are not included as their output voltage would be zero); the results for the vertical compression and lateral stretch are summarized in the last two rows of Table 1.

In a case of a lateral bending with force applied at the free tip of the nanowire, since the highest strain is located in the bottom, nanowires with BT contact are not optimal from the point of view of the piezoelectric potential generated by a given force. This conclusion is consistently confirmed by all our FEM simulations. However, in a case of vertical compression, even if both the BT and TT contacts are present, a relatively large potential can still be generated; besides, though the strain mechanical energy is much smaller, the parameter ξ is significantly higher. Moreover, laterally stretched wires can produce high output potentials even if both their ends have total metal contacts, a striking advantage from the point of view of practical implementations, in excellent agreement with recently reported experimental results [7].

Fig. 6. Piezoelectric potential distribution (side view) of a laterally stretched piezoelectric nanowire.
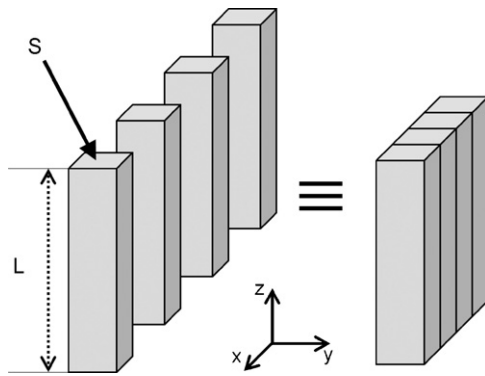
Fig. 7. Schematic representation of the equivalence between many nanowires connected in parallel and a single nanowall.

When the nanowire is laterally bent, the differential potential between the compressed and stretched sides is almost independent on the height of the nanowire. On the other hand, when the nanowire is vertically compressed, the potential generated between the top and bottom surfaces is directly proportional to the height of the nanowire and is independent on the cross-section dimensions of the nanowire itself. Instead, in the lateral stretch case, the potential between top and bottom contact is inversely proportional to the cross-section dimensions of the nanowire.

It must be pointed out that the ξ parameter defined here is only a parameter for characterizing the ratio of electrostatic energy to total input mechanical energy. It is not the efficiency of the nanogenerator, because the nanowires will experience many cycles of vibrations after the force action, and in each cycle, there is no input mechanical energy but with electrical energy output.

4. Bent nanowall

A nanowall can also be used for energy harvesting; neglecting technological issues and second order effects, this structure would be equivalent to a large number of parallel nanowires connected in parallel, thus increasing the maximum output current.
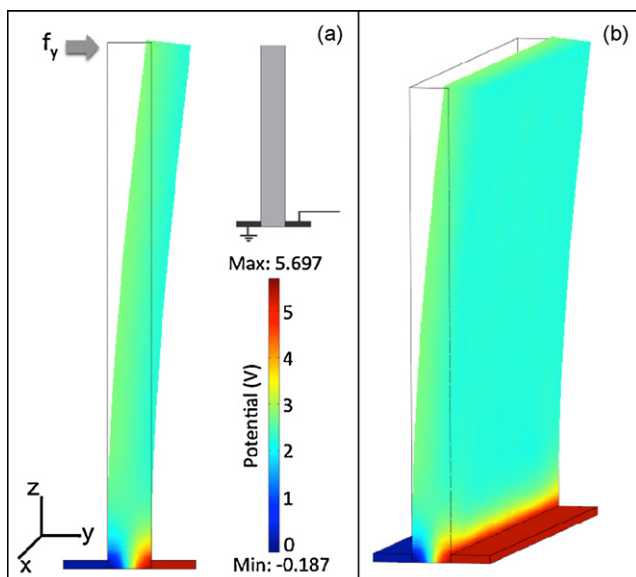
Fig. 8. Potential distribution of a bent bottom-bottom nanowall; (a) is a side view; (b) is a 3D view.

This result can be understood by considering the parallel connection of N identical two-terminal devices, as schematically shown in Fig. 7. In fact, if, as a simple example, we consider a uniform conductor with regular cross-section S, if the current flow is parallel to the axis z, the electrical resistance is given by $R = \rho L/S$ where ρ is the electrical resistivity, L is the length of the conductor and S is the section; if N such identical resistors are connected in parallel, the total resistance would be $\rho L/NS$; the same result is found if, starting with the same N identical resistors in parallel, we "merge" these N identical resistors into a single resistor with length L and cross-section NS (see Fig. 7). Similarly, with reference to Fig. 7, the parallel connection of N identical photo-voltaic cells, each with section S, is equivalent to a single photo-voltaic cell with section NS (i.e. with a maximum current N times higher). In the same manner, with reference to Figs. 1 and 7, if the input force is parallel to the "merging" surfaces of the nanowires (i.e. if the input force is orthogonal to the axis x), the connection of N identical nanowires is equivalent to a single nanowall with section N times bigger (this result applies for all possible positions of the contacts shown in Fig. 1, provided the nanowires are completely identical, i.e., they also have identical contacts and input mechanical force). Obviously, the possible contact configurations for nanowalls are the same as for nanowires and the same conclusions apply (see the previous section). Here, for simplicity, we only show the FEM simulation of a BL–BR ZnO laterally bent nanowall.

The nanowall has the same cross-section height (600 nm) and side (50 nm) of the nanowires considered in the previous section and a depth of 600 nm. The two lateral contacts were extended too, as shown in Fig. 8b and, clearly, the mechanical force has been properly scaled so that the same deformation is obtained (i.e., the same surface force has been considered).

The potential distribution has been calculated under the same boundary conditions of the previous simulation (BL contact grounded) and the results show a differential potential of about 6 V between the BL and BR contacts.

The electrostatic energy for this configuration is 4.87×10^{-16} J, which is close to the electrostatic energy which would be obtained by a correspondent number of "isolated" nanowires. The strain energy is 5.17×10^{-14} J; the parameter ξ is 0.0094 (which is close to the values of the same parameter for the correspondent bottom-bottom nanowires).

5. Conclusions

We have investigated the static piezoelectric potential in nanowires; our results provide insight for understanding previously reported experimental results and guidelines for the design of high-efficiency piezoelectric nanogenerators; in particular, we have shown that the piezoelectric potential mechanically induced in a deformed nanostructure can critically depend on the position and dimensions of the metal contacts and on the way the input force is applied. For this reason, we have classified and systematically compared the most important configurations for piezoelectric nanostructures, showing, in particular, that laterally stretched wires have important practical advantages as they can generate high output potentials even when both their ends present two "total contacts", in agreement with experimental results in [7]. Finally, we have suggested nanowalls for effectively increasing the output current; even for nanowalls, vertical compression and lateral stretching are possible and, in case of lateral bending, contacts near high-strain regions should, if possible, be avoided. Our theoretical results are consistently confirmed by FEM simulations and can guide the development of high-efficiency piezoelectric structures for energy harvesting.

Acknowledgment

References

[1] K.A. Cook-Chennault, N. Thambi, A.M. Sastry, Powering MEMS portable devices—a review of non-regenerative and regenerative power supply systems with special emphasis on piezoelectric energy, Smart Mater. Struct. 17 (2008) 043001.

[2] Z.L. Wang, J. Song, Piezoelectric nanogenerators based on zinc oxide nanowire arrays, Science 312 (14 April 2006).

[3] X. Wang, J. Song, Z.L. Wang, Direct-current nanogenerator driven by ultrasonic waves, Science 316 (6 April 2007).

[4] P.X. Gao, J. Song, J. Liu, Z.L. Wang, Nanowire piezoelectric nanogenerators on plastic substrates as flexible power sources for nanodevices, Adv. Mater. 19 (2007) 67–72.

[5] Z.L. Wang, Self powered nanotech, Scientific American (January) (2008) 82–87.

[6] Y. Qin, X. Wang, Z.L. Wang, Microfibre-nanowire hybrid structure for energy scavenging, Nature 451 (February) (2008).

[7] R. Yang, L. Qin, L. Dai, Z.L. Wang, Power generation with laterally packaged piezoelectric fine wires, Nat. Nanotech. (November) (2008), AOP.

[8] Y. Gao, Z.L. Wang, Electrostatic potential in a bent piezoelectric nanowire. The fundamental theory of nanogenerators and nanopiezotronics, Nano Lett. 7 (8) (2007).

[9] Z.L. Wang, Towards self-powered nanosystems: from nanogenerators to nanopiezotronics, Adv. Funct. Mater. 18 (2008) 1–15.

[10] X. Wang, J. Song, Z.L. Wang, Single-crystal nanocastles of ZnO, Chem. Phys. Lett. 424 (2006) 86–90.

[11] C. Falconi, A. D'Amico, Z.L. Wang, Wireless Joule nanoheaters, Sens. Actuators B 127 (2007) 54–62.

[12] C. Falconi, A. D'Amico, Z.L. Wang, Wireless nanoactuators and nanosensors for in-vivo biomedical application, in: Proceedings of Eurosensors XX, Goteborg, Sweden, 2006.

[13] C. Falconi, E. Martinelli, C. Di Natale, A. D'Amico, F. Maloberti, P. Malcovati, A. Baschirotto, V. Stornelli, G. Ferri, Electronic interfaces, Sens. Actuators, B: Chem. 121 (January (1)) (2007) 295–329.

[14] C. Loo, A. Lin, L. Hirsch, M.H. Lee, J. Barton, N. Halas, J. West, R. Drezek, Nanoshell-enabled phtonics-based imaging and therapy of cancer, Technol. Cancer Res. Treatment 3 (2004) 33–40.

[15] S.R. Sershen, S.L. Westcott, N.J. Halas, J.L. West, Temperature-sensitive polymer-nanoshell composites for photothermally modulated drug delivery, J. Biomed. Mater. Res. 51 (2000) 293–298.

Biographies

Christian Falconi was born in Rome, Italy, 1973. He received the MSc (cum laude) and the PhD degrees in electronic engineering from the University of Tor Vergata, Rome, Italy, in, respectively, 1998 and 2001; as a part of his PhD program he visited the University of Linkoping (1 month), and TU Delft (7 months). In 2002 he has supervised the design of the electronic interface for the ST-Microelectronics DNA chip. Since 2002 Christian Falconi is assistant professor at the Department of Electronic Engineering, University of Tor Vergata, where he teaches Low Voltage Analog Electronics and Fundamental of Electronics. Since 2003 he has been visiting the Georgia Institute of Technology (10 months). He authored or co-authored 40 papers on international journals and conference proceedings. His research interests include electronic devices, analog circuits, electronic interfaces, sensors, microsystems, and nanosystems.

Giulia Mantini was born in Italy, 1982. She received the MSc (cum laude) degree in Medical Engineering from the University of Tor Vergata, Rome, Italy, in 2007 and is currently a PhD student (Microsystem Engineering) at the same University. She is currently visiting student researcher (Fulbright Scholar) at the Georgia Institute of Technology. Her research interests include sensors, microsystems, nanosystems for medical applications, and FEM simulations of micro/nano-structures.

Arnaldo D'Amico received the Laurea degree in physics and electronic engineering from the University La Sapienza, Rome, Italy. For several years, he has been with the National Research Council (CNR) leading the Semiconductors Laboratory at the Solid State Electronic Institute, Rome. In 1986, he was appointed full professor of electronics at the University of L'Aquila, and, since 1990, he has been with the University of Rome Tor Vergata where he leads the Sensors and Microsystems Group and is full professor of electronics, Faculty of Engineering. He teaches courses on electronic devices, microsystems, and sensors. Currently, his main research activities are concerned with the development of physical and chemical sensors, low voltage electronics, noise, and advanced electronic devices. He is author of more than 450 papers in international journals and conference proceedings. He has been chairman of several conferences on sensors, electronics, and noise and a member of the editorial board of the journals Sensors and Actuators A (physical) and Sensors and Actuators B (chemical). He served as Chairman of the Steering Committee of the Eurosensors conference series from 1999 to 2004. At the national level, he is chairman of the National Society of Sensors and Microsystems (AISEM) and Director of the Institute of Acoustics "O. M. Corbino" of the National Research Council (CNR).

Zhong Lin Wang received the BS degree in Applied Physics from the Northwest Telecommunication Engineering Institute, China, in 1982, and the PhD degree in Physics from the Arizona State University in 1987. Subsequently, he was visiting lecturer at the Department of Material Science & Engineering, The State University of New York at Stony Brook (September 1987–September 1988); research fellow at the Cavendish Laboratory, University of Cambridge, England (October 1988–October 1989); research fellow at the U.S. Department of Energy, Research Fellowship, Metals and Ceramics Division, Oak Ridge National Laboratory (November 1989–September 1990); research associate professor at the Metals and Ceramics Division, Oak Ridge National Laboratory and Department of Materials Science, the University of Tennessee (September 1990-April 1993); research scientist at the National Institute of Standards and Technology (December 1993–February 1995). Since March 1995 he is with the School of Materials Science and Engineering, Georgia institute of Technology, where he currently is Regents' Professor, COE Distinguished Professor, and Director of the Center for Nanostructure Characterization and Fabrication. Wang has published over 480 articles in peer-reviewed journals, which have defining influence on the field of nanotechnology as evidenced by high citation (>27,000 times) and impact factor (his h-index is 78). Among other achievements, Dr. Wang and his group have first reported nanobelts of semiconducting oxides; self-assembled, single-crystal nanorings and nanohelixes; piezoelectric nanogenerators.